ARTICLE

ACS chemical biology

Antagonism of c-IAP and XIAP Proteins Is Required for Efficient Induction of Cell Death by Small-Molecule IAP Antagonists

Chudi Ndubaku[†], Eugene Varfolomeev[†], Lan Wang, Kerry Zobel, Kevin Lau, Linda O. Elliott, Brigitte Maurer, Anna V. Fedorova, Jasmin N. Dynek, Michael Koehler, Sarah G. Hymowitz, Vickie Tsui, Kurt Deshayes, Wayne J. Fairbrother*, John A. Flygare*, and Domagoj Vucic*

Departments of Medicinal Chemistry and Protein Engineering, Genentech, Inc., South San Francisco, California 94080, [†]These authors contributed equally to this work.

ABSTRACT The inhibitor of apoptosis (IAP) proteins are critical regulators of cancer cell survival, which makes them attractive targets for therapeutic intervention in cancers. Herein, we describe the structure-based design of IAP antagonists with high affinities and selectivity (>2000-fold) for c-IAP1 over XIAP and their functional characterization as activators of apoptosis in tumor cells. Although capable of inducing cell death and preventing clonogenic survival, c-IAP-selective antagonists are significantly less potent in promoting apoptosis when compared to pan-selective compounds. However, both pan-IAP- and c-IAP-selective antagonists stimulate c-IAP1 and c-IAP2 degradation and activation of NF-κB pathways with comparable potencies. Therefore, although compounds that specifically target c-IAP1 and c-IAP2 are capable of inducing apoptosis, antagonism of the c-IAP proteins and XIAP is required for efficient induction of cancer cell death by IAP antagonists.

Programmed cell death, or apoptosis, is a genetically regulated cell suicide mechanism that plays a major role in development and homeostasis in metazoans (*1*). Insufficient apoptosis can lead to the development and progression of human cancers (*2, 3*). Apoptotic cell death can be initiated through the engagement of cell-surface pro-apoptotic receptors by their specific ligands or by changes in internal cellular integrity (*4, 5*). Both of these pathways converge at the activation of effector caspases (*6*). Caspases are cysteine-dependent aspartyl-specific proteases that comprise the effector arm of apoptotic cell death (*6*). Blockade of programmed cell death enhances cell survival and contributes to escape from cytotoxic therapies (*7*); the inhibitor of apoptosis (IAP) proteins contribute significantly to this phenomenon (*8*).

Originally identified over 15 years ago in baculoviruses, IAP proteins are now known in both invertebrates and vertebrates (*9, 10*). The IAP proteins are characterized by one to three tandem baculovirus IAP repeat (BIR) domains, and most of them also possess a carboxy-terminal ubiquitin ligase RING domain (*9, 11*). Cellular IAP proteins, c-IAP1 and c-IAP2, were identified through their ability to interact with tumor necrosis factor receptor-associated factor 2 (TRAF2) (*12*). This unique property among IAP proteins enables recruitment of c-IAP1 and c-IAP2 to TNFR-signaling complexes where they regulate the activation of caspase-8 (*12, 13*). X-Chromosome-linked IAP (XIAP) is a potent antiapoptotic protein as a result of its potent inhibition of caspases (*6*). For inhibition of caspases 3 and 7, XIAP utilizes its BIR2 domain, as well as the linker between

***Corresponding authors,**
fairbro@gene.com,
jflygare@gene.com,
domagoj@gene.com.

Received for review April 6, 2009 and accepted June 3, 2009.

Published online June 3, 2009

10.1021/cb900083m CCC: $40.75

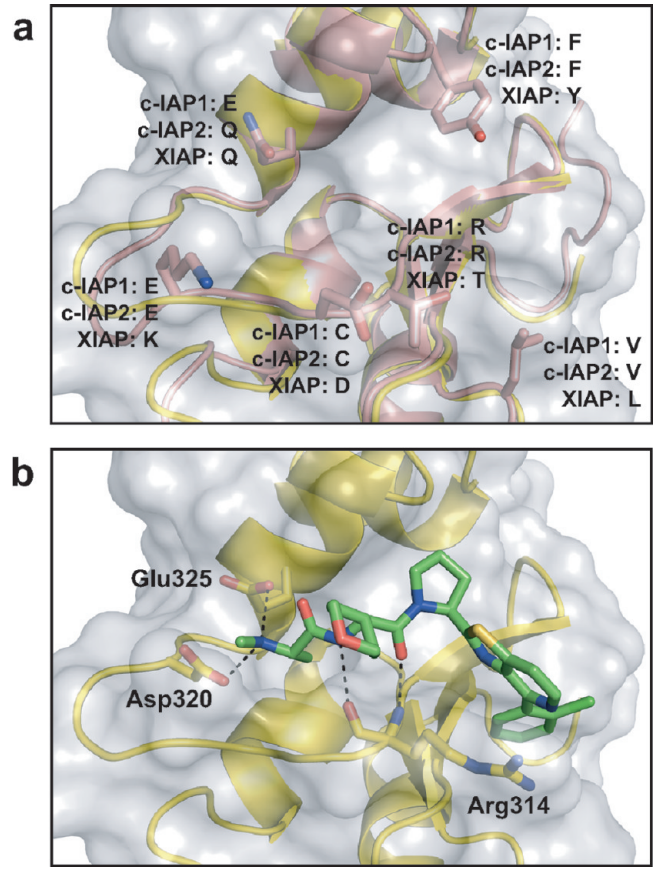

Figure 1. IAP antagonist binding site. a) Molecular surface representation of IAP antagonist-binding groove of the c-IAP1 BIR3 domain; also shown are ribbon representations of c-IAP1 (yellow) and XIAP (pink) BIR3 domains. Highlighted residues indicate the differences between the indicated IAP proteins. The residue positions are as follows (starting from the bottom right of the figure and going clockwise): 1) c-IAP1: V298, c-IAP2: V284, XIAP: L292; 2) c-IAP1: R314, c-IAP2: R300, XIAP: T308; 3) c-IAP1: C315, c-IAP2: C301, XIAP: D309; 4) c-IAP1: E317, c-IAP2: E303, XIAP: K311; 5) c-IAP1: E325, c-IAP2: Q311, XIAP: Q319; 6) c-IAP1: F330, c-IAP2: F316, XIAP: Y324. b) Structural model of PS1 (green) with the BIR3 domain of c-IAP1. Dashed lines indicated hydrogen bond interactions with highlighted residues of c-IAP1.

BIR1 and BIR2 (*14*). For caspase-9 inhibition, a peptide-binding groove on the surface of the BIR3 domain interacts with a conserved four-residue IAP-binding motif (IBM) exposed at the amino terminus of the small subunit of processed caspase-9 (*15, 16*).

The antiapoptotic activity of IAP proteins can be antagonized by the second mitochondrial activator of caspases (SMAC) (*17, 18*). Various death stimuli trigger proteolytic processing and subsequent release of SMAC from mitochondria into the cytoplasm (*17, 18*). SMAC processing exposes an IBM (AVPI) that binds the peptide-binding groove on the surface of the BIR domains of IAP proteins (*19–21*). A number of IAP antagonists that mimic SMAC amino-terminal peptides and disrupt IAP binding to activated caspase-9 and SMAC have been reported (*22–29*). These IAP antagonists trigger apoptosis in cancer cells and inhibit tumor growth *in vivo*. Binding of IAP antagonists leads to induction of c-IAP autoubiquitination activity and rapid proteasomal degradation of the c-IAP proteins (*30–32*). Besides neutralizing these antiapoptotic proteins, the IAP antagonists activate canonical and non-canonical NF-κB pathways and induce cell death that is dependent on TNF signaling (*30–34*). The activation of NF-κB pathways by IAP antagonists is dependent on them binding to the BIR3 domains of c-IAP1 and 2 and thereby inducing c-IAP ubiquitin ligase activity (*30–32, 35, 36*).

Small-molecule IAP antagonists reported to date generally have high affinities for the BIR3 domain of XIAP as well as the BIR3 domains of c-IAP1 and 2. To elucidate the relative importance of c-IAP targeting for IAP antagonist induced apoptosis and cellular signaling, we designed c-IAP-selective antagonists. Such c-IAP-selective antagonists induce cancer cell apoptosis, but the efficiency of this cell killing is significantly reduced in comparison to that of pan-selective IAP antagonists. This is despite the fact that c-IAP-selective antagonists stimulate c-IAP1 and c-IAP2 protein degradation and activation of NF-κB pathways to an extent that is comparable to the pan-selective molecules. In long-term survival assays, pan-selective IAP antagonists were also more efficient than c-IAP-selective compounds, suggesting that antagonism of the c-IAP proteins and XIAP is needed for efficient cell death induction by IAP antagonists. This study provides a functional analysis of c-IAP antagonism and further validation of targeting IAP proteins for the treatment of cancer.

RESULTS AND DISCUSSION

Structure-Based Design of a c-IAP-Selective Antagonist. To examine the therapeutic potential and biological consequence of c-IAP antagonism, structure-based design was used to generate novel compounds that selectively target the c-IAP1 and c-IAP2 proteins. Analysis of the overlay of the IAP antagonist/SMAC peptide-binding sites for the BIR domains of interest (XIAP BIR3, c-IAP1 BIR3, and c-IAP2 BIR3) revealed a

TABLE 1. Structures of IAP antagonists and binding affinities for XIAP-BIR3, c-IAP1-BIR3, and c-IAP2-BIR3

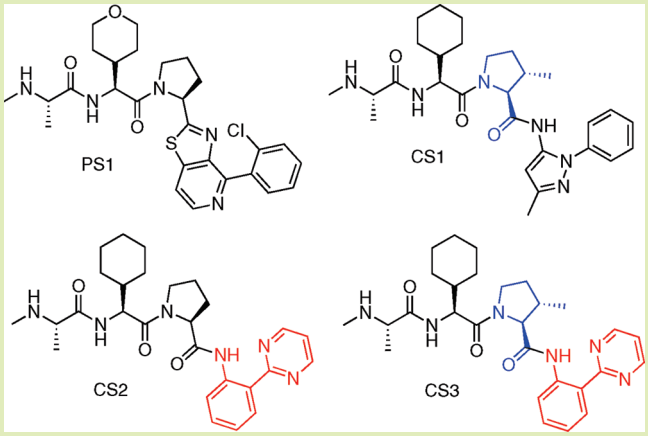

	K_i (μM)[a]			
Antagonist	c-IAP1 BIR3	c-IAP2 BIR3	XIAP BIR3	Selectivity (X/c1)
PS-1	0.036	0.096	0.033	~1
ent-PS-1	>34	>34	>34	ND
CS-1	0.010	0.052	2.4	240
CS-2	0.037	0.114	5.05	137
CS-3	0.016	0.085	>34	>2000

[a]All results are an average of at least two experiments. ND = not determinable.

number of key residue variations that could be exploited to impart selectivity (Figure 1, panel a) (*19–21*). Unfortunately, the majority of these variations exist in the solvent-exposed regions of the IAP antagonist-binding surfaces. We found that targeting these peripheral residues did not result in enhanced selectivity, presumably because of large desolvation penalties that the IAP antagonists needed to overcome. Pan-selective IAP antagonists (*i.e.*, PS1, Table 1) make a number of dipolar as well as hydrophobic interactions deep within the binding surfaces of the BIR domains (Figure 1, panel b). One key difference within this hydrophobic cleft that we utilized effectively was Tyr324 in XIAP BIR3 *versus* Phe330 in c-IAP1 BIR3. The steric environment created by the hydroxyl functional group on this residue of XIAP and absent in c-IAP1 created intolerance for substituents on the compound that were in proximity to this residue of XIAP BIR3 (Figure 2); similar observations were made previously when comparing the binding of antagonists to the single BIR domain of ML-IAP and XIAP BIR3 (*37*). This sensitivity is illustrated in CS1, a compound with a methyl substituent on the P3 region (colored blue) that has significantly higher affinity for c-IAP1 BIR3 over XIAP BIR3 (240-fold) compared to the pan-selective PS1 lacking this substituent (Table 1).

Orthogonally, an increase in selectivity was uncovered by the insertion of a 2-pyrimidinyl substituent at the P4 region (colored red) of these IAP antagonists. We hypothesized that this moiety would impart selectivity by exploiting electronic and steric differences between the XIAP and c-IAP BIR3 P4 binding sites. In XIAP BIR3, a lone pair-lone pair repulsion is expected between the hydroxyl functional group of Thr308 and one of the nitrogen atoms within the 2-pyrimidinyl heterocycle (Figure 2, panel a). The corresponding residue in c-IAP1 BIR3 is Arg314, whose side chain methylene group is not capable of similar electronic repulsion (Figure 2, panel b). In addition, the XIAP BIR3 P4 pocket is slightly smaller than the c-IAP1 BIR3 P4 pocket as a result of the presence of Leu292 (*versus* Val298 in c-IAP1) at the base of the pocket. This difference may impair binding to XIAP BIR3 by compounds with bulky P4 substituents. Thus the pyrimidinyl functional group was expected to disfavor XIAP BIR3 binding because of suboptimal interactions with both Thr308 and Leu292. Indeed, when CS2 containing this 2-pyrimidinyl substituent was synthesized and examined, it had high selectivity (137-fold) for c-IAP1 BIR3 over XIAP BIR3 as well (Table 1). Not surprisingly, incorporating this selectivity element into an antagonist bearing the P3 methyl substituent that also enabled c-IAP1 selectivity (CS1) resulted in CS3, a compound with high affinity ($K_i < 20$ nM) and selectivity (>2000-fold) for c-IAP1 BIR3 over XIAP BIR3 (Table 1). Consistent with our design hypothesis, the X-ray crystal structure of CS3 in complex with XIAP BIR3 revealed that the pyrimidinyl group does not interact with the P4 pocket but rather is exposed to the

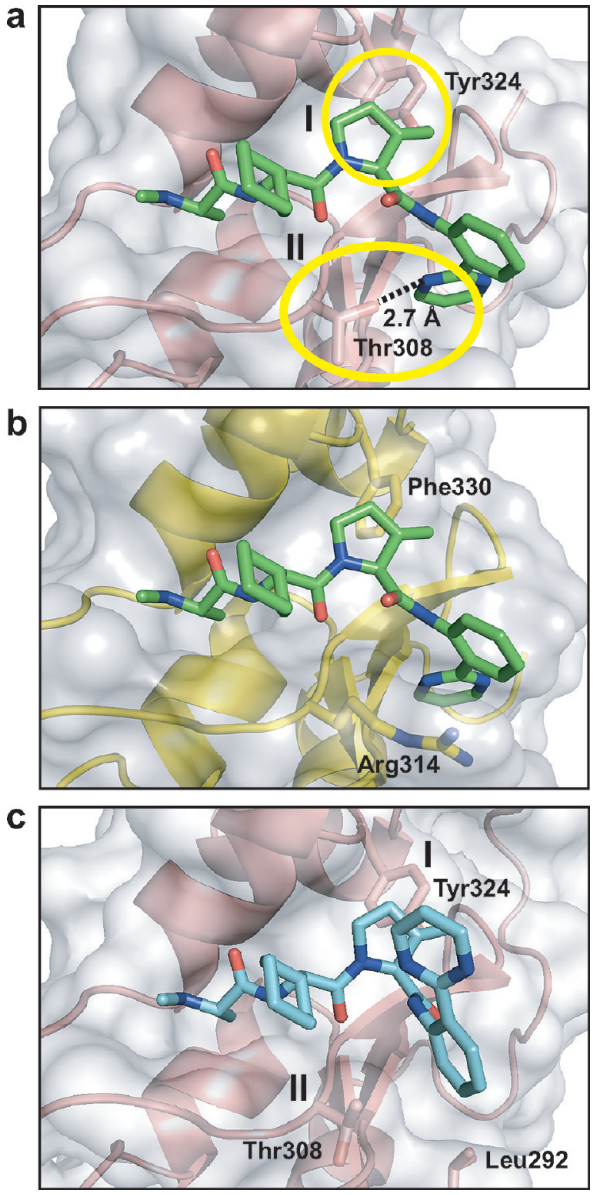

Figure 2. Structural models of CS3 (green) with the BIR3 domains of XIAP (pink) (a) and c-IAP1 (yellow) (b) with highlighted steric clashes of CS3 with Tyr324 (I) and electronic repulsion of CS3 with Thr308 (II) of XIAP (a). Corresponding residues for c-IAP1 are highlighted in panel b. (c) 1.8 Å resolution X-ray crystal structure of CS3 (cyan) in complex with the BIR3 domain of XIAP shows the 2-pyrimidinyl moiety does not bind in the XIAP BIR3 P4 pocket and validates the selectivity design hypothesis.

solvent (Figure 2, panel c). Therefore, by utilizing structural differences in the IAP antagonist-binding groove on the surface of the BIR3 domains of the c-IAP proteins and XIAP, we have generated antagonists with high affinity and selectivity for c-IAP1 and c-IAP2.

c-IAP-Selective Antagonist Does Not Disrupt XIAP Protein Complexes. Physical interactions of IAP proteins with caspases and SMAC are critical for their anti-apoptotic activity (*38*). To investigate the effect of a c-IAP-selective antagonist on these protein−protein interactions, CS3 and PS1 were added to cellular lysates prepared from cells transfected with XIAP or c-IAP1 and caspase-9 or SMAC (Figure 3). While XIAP BIR3-binding pan-selective IAP antagonist compound PS1 prevented XIAP:caspase-9 association at all concentrations tested, the c-IAP-selective compound CS3 showed no effect at lower concentrations and only partial inhibition of this protein−protein interaction at the highest concentration tested (25 μM) (Figure 3, panel a). Similarly, PS1 efficiently blocked XIAP:SMAC association, whereas CS3 demonstrated a disruptive effect only at the highest concentration tested (Figure 3, panel b).

In contrast to the effect on XIAP BIR3-mediated interactions, CS3 completely abrogated c-IAP1:SMAC association at all experimental concentrations (Figure 3, panel c). The enantiomer of PS1, *ent*-PS1, did not show any appreciable effect on these XIAP- or c-IAP1-mediated protein−protein interactions (Figure 3, panels a−c) in agreement with its inability to bind XIAP and c-IAP1 BIR3 domains. Therefore, the c-IAP-selective antagonist can efficiently disrupt c-IAP1 protein complexes but not the association of XIAP with caspase-9 or SMAC.

Pan-Selective IAP Antagonist Is a More Potent Inducer of Cell Death than c-IAP-Selective Antagonist. To evaluate the ability of pan-IAP and c-IAP-selective antagonists to induce cell death, EFM-192A, EVSA-T, and A2080 cancer cell lines were treated with PS1 or CS3 (Figure 4). Both IAP antagonists exhibited single-agent cell killing activity (Figure 4, panel a and Supplementary Figure 1). However, PS1 was substantially more efficient than CS3 in stimulating apoptosis, with approximate IC_{50} values of 15 nM for PS1 and 150 nM for CS3, in the highly sensitive EVSA-T cell line (Figure 4, panel a). The enantiomer compound *ent*-PS1 did not induce any appreciable cell death (Supplementary Figure 2). This differential pro-apoptotic activity was also evident in a caspase-3/7 activation assay as PS1 stimulated significantly higher caspase activity compared to that of CS3 (Figure 4, panel b).

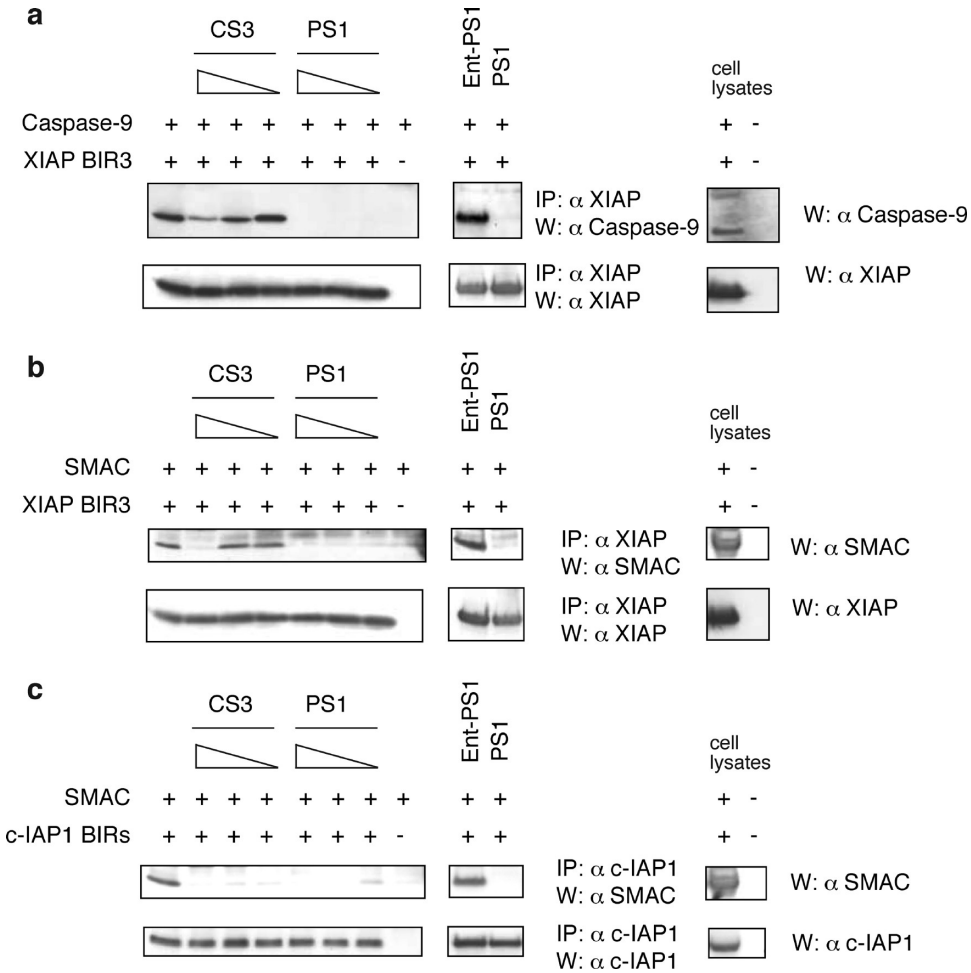

Figure 3. c-IAP-selective antagonist CS3 disrupts c-IAP1 but not XIAP protein complexes. 293T cells were transiently co-transfected with caspase-9 and Flag-tagged XIAP-BIR3 constructs (a), SMAC and Flag-tagged XIAP-BIR3 (b), or SMAC and Flag-tagged c-IAP1-BIR1-3 constructs (c). After 40 h, cells were lysed in NP-40 lysis buffer. The cellular lysates were incubated with the indicated IAP antagonists at 25, 2.5, or 0.25 μM concentration for 2 h and then immunoprecipitated with the anti-Flag affinity resin for 3 h. *ent*-PS1 and PS1 were used at 25 μM in the middle panels. Protein associations and expression were determined by Western blotting with anticaspase-9, anti-SMAC, and anti-Flag antibodies.

IAP antagonist-induced cell death depends on caspase-8 activation and TNF signaling (*31–34*). Therefore, we wanted to examine if cell death induced by the c-IAP-selective antagonist also relies on TNFR1-mediated signaling. Treatment of cell with CS3 or PS1 induced comparable activation of caspase-8 activity (Figure 4, panel c). In addition, the presence of TNFR1-Fc but not the combination of DR5-Fc and Fas-Fc protected cells from CS3- or PS1-induced apoptosis (Figure 4, panel d), confirming the importance of the TNFR1-mediated signaling pathway for IAP antagonist-induced cell death. In agreement with earlier reports, caspase inhibition efficiently blocked CS3- and PS1-induced apoptosis (Supplementary Figure 3).

The ability of c-IAP-selective and pan-selective IAP antagonists to prevent long-term cellular survival was also examined in a clonogenic assay. High concentrations of compounds prevented colony formation, but lower concentrations allowed differentiation between the more potent pan-selective IAP compound PS1 and the c-IAP-selective compound CS3, demonstrating that antagonism of both c-IAP proteins and XIAP is much more effi-

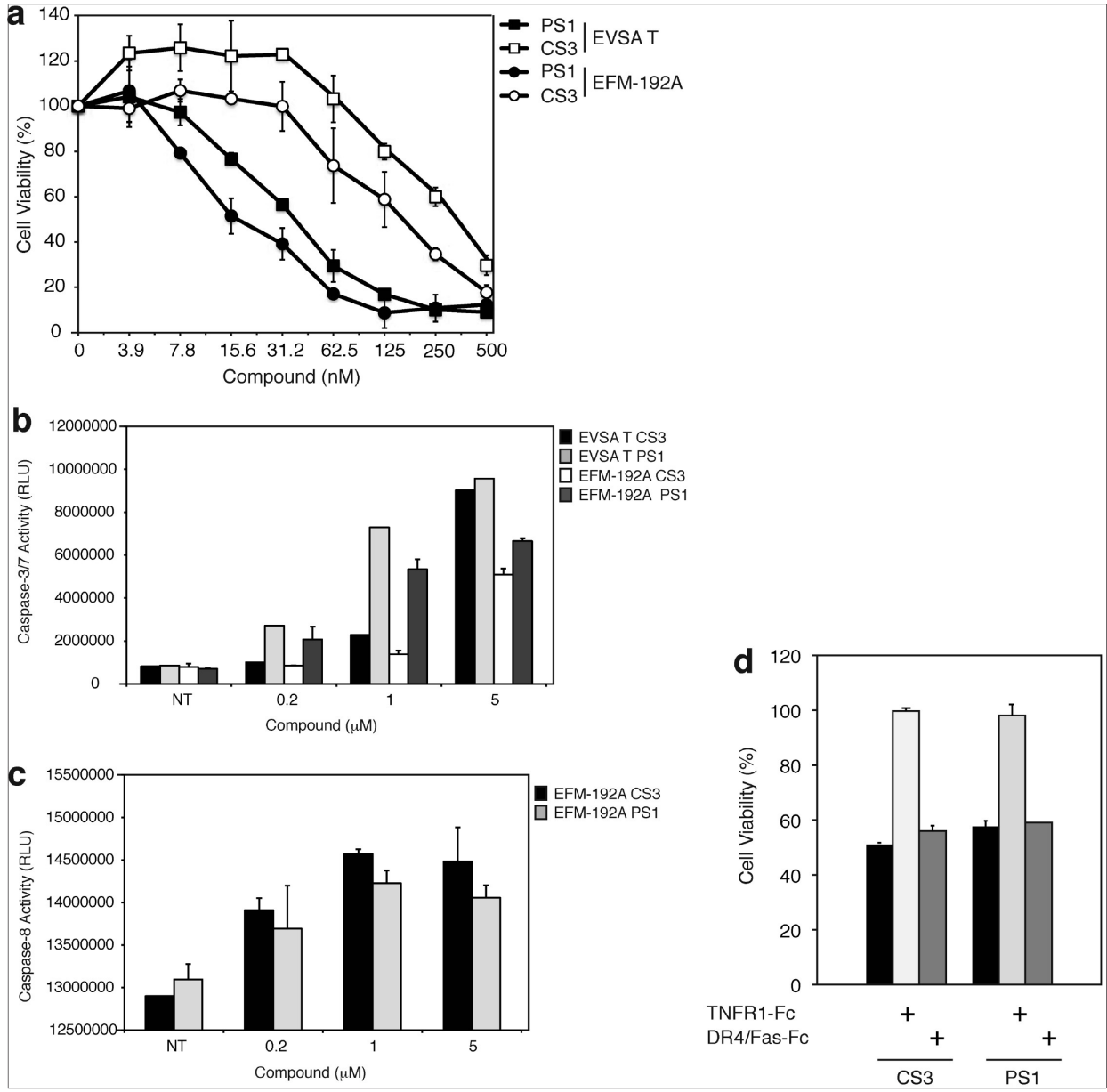

Figure 4. Cell death induction by c-IAP-selective and pan-selective IAP antagonists. a) EFM-192A and EVSA-T cells were treated with increasing concentrations of PS1 or CS3 for 24 h. Cell viability was determined as described in Methods. b, c) Indicated cell lines were treated with PS1 or CS3 for 5 h and caspase-3/7 (b) or caspase-8 (c) activation was assessed as described in Methods. d) Cell death induction by c-IAP-selective antagonist is dependent on TNF. A2058 cells were treated with CS3 (1 μM) or PS1 (50 nM) alone or in the presence of the TNFR1-Fc or Fas-Fc/DR5-Fc (5 μg mL^{-1}) for 24 h. Cell viability was determined as described in Methods.

cacious in precluding clonogenic cellular survival (Figure 5, panel a). Inhibition of caspase activity and TNF signaling afforded protection to cells from PS1- and CS3-induced cell death and allowed for long-term survival (Figure 5, panel b and data not shown). These results suggest that antagonism of c-IAP proteins without targeting XIAP is not sufficient for efficient induction of apoptosis by IAP antagonists. Nevertheless, cell death induced by pan-selective or c-IAP-selective IAP antagonists proceeds through TNF signaling and caspase activation.

c-IAP-Selective Antagonist Triggers c-IAP1 and c-IAP2 Degradation and NF-κB Activation. IAP antagonists stimulate the ubiquitin ligase activities of c-IAP1 and c-IAP2 leading to the activation of canonical and non-canonical NF-κB signaling and the proteasomal degradation of c-IAP1 and c-IAP2 (*30–32*). However, these earlier studies used nonselective, pan-selective IAP antagonists (*30–32*). To examine whether antagonism of c-IAP proteins is sufficient for IAP antagonist-mediated NF-κB activation and c-IAP1 degradation, cells were treated with PS1 or CS3 (Figure 6). Both PS1 and

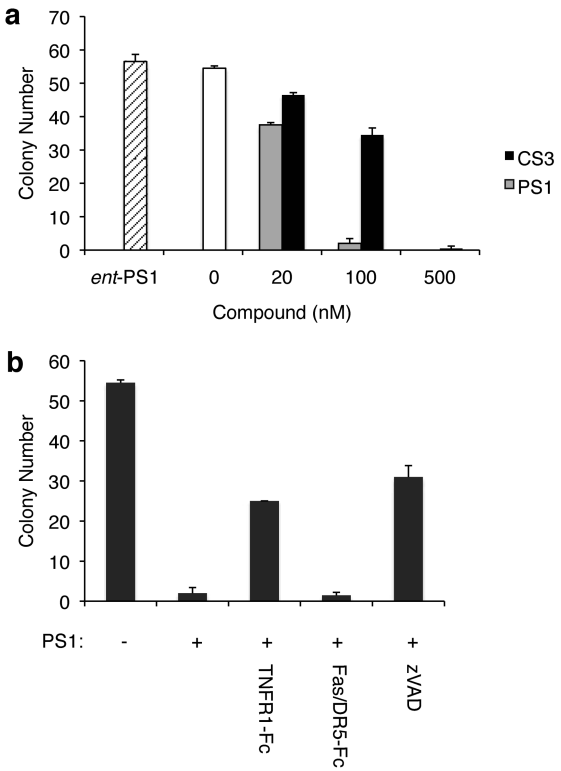

Figure 5. Prevention of clonogenic survival by c-IAP-selective antagonist. a) EFM-192A cells were treated with the indicated concentrations of CS3, PS1, or PSE1 or solvent control and then plated. The average number of colonies was determined 10 days later. b) Blockade of TNF signaling allows long-term clonogenic survival of IAP antagonist-treated cells. EFM-192A cells were treated with PS1 (100 nM) in the absence or presence of zVAD (20 μM), TNFR1-Fc (5 μg mL^{-1}), or DR5-Fc and Fas-Fc (5 μg mL^{-1}), plated, and subsequently assessed as in panel a.

CS3 triggered degradation of c-IAP1 and c-IAP2 in similar fashions (Figure 6, panels a and b, and Supplementary Figure 4). Administration of PS1 and CS3 also stimulated activation of canonical (Figure 6, panel a) and non-canonical NF-κB signaling (Figure 6, panel b). This NF-κB activation resulted in comparable stimulation of *TNFα* and *MCP1* mRNA expression (Figure 6, panel c). At the same time, *ent*-PS1 did not cause any c-IAP1 and c-IAP2 degradation or NF-κB activation (Supplementary Figures 4 and 5). Therefore antagonism of c-IAP proteins is sufficient for the stimulation of c-IAP protein degradation and NF-κB activation. These data further establish that IAP antagonist-stimulated activation of NF-κB signaling does not require XIAP; instead it relies on c-IAP1 and c-IAP2.

The ability of IAP proteins to inhibit apoptosis and promote cellular survival pathways, combined with their elevated expression in human malignancies, makes these proteins attractive targets for therapeutic intervention (*39*). Equally important, the interactions of IAP proteins with pro-apoptotic proteins can be prevented using SMAC-mimicking IAP antagonists, thus demonstrating the feasibility of targeting IAP proteins. Mechanistic studies on IAP antagonist-stimulated cellular responses revealed that these reagents trigger proteasomal degradation of c-IAP1 and c-IAP2, activation of canonical and non-canonical NF-κB pathways, and cell death that depends on TNFR1-mediated signaling (*40*). Most efforts to identify small-molecule antagonists of IAP proteins have targeted the BIR3 domains of XIAP, c-IAP1, and c-IAP2. The IAP antagonists reported to date target indiscriminately the BIR3 domains of multiple IAP proteins (*41*). Our pan-selective antagonist, PS1, also binds to the BIR3 domains of the examined IAP proteins with similar affinities. Using structure-based design, we sought to maintain an equivalent affinity of antagonists for c-IAP1 BIR3 while disrupting the binding to XIAP BIR3. This led to the generation of CS1, a compound with a methyl group designed to interact favorably with the side chain of c-IAP1 BIR3 residue Phe330 but negatively with Tyr324 of XIAP-BIR3. Further investigation revealed that a pyrimidine ring in the P4 position of IAP antagonists resulted in significant electronic and steric repulsion with XIAP BIR3 but that this ring can be accommodated in the P4 pocket of c-IAP BIR3. Ultimately, the combination of these two selectivity elements resulted in the production of CS3, a compound with high affinity and selectivity for c-IAP1 and c-IAP2.

Although structurally similar, XIAP and the c-IAP proteins regulate apoptosis in distinct fashions. While XIAP directly binds and inhibits caspases 3, 7, and 9, c-IAP1 and c-IAP2 regulate activation of caspase-8 in TNFR1-mediated signaling complexes (*14, 30–32, 34*). IAP antagonist-induced proteasomal degradation of c-IAP1

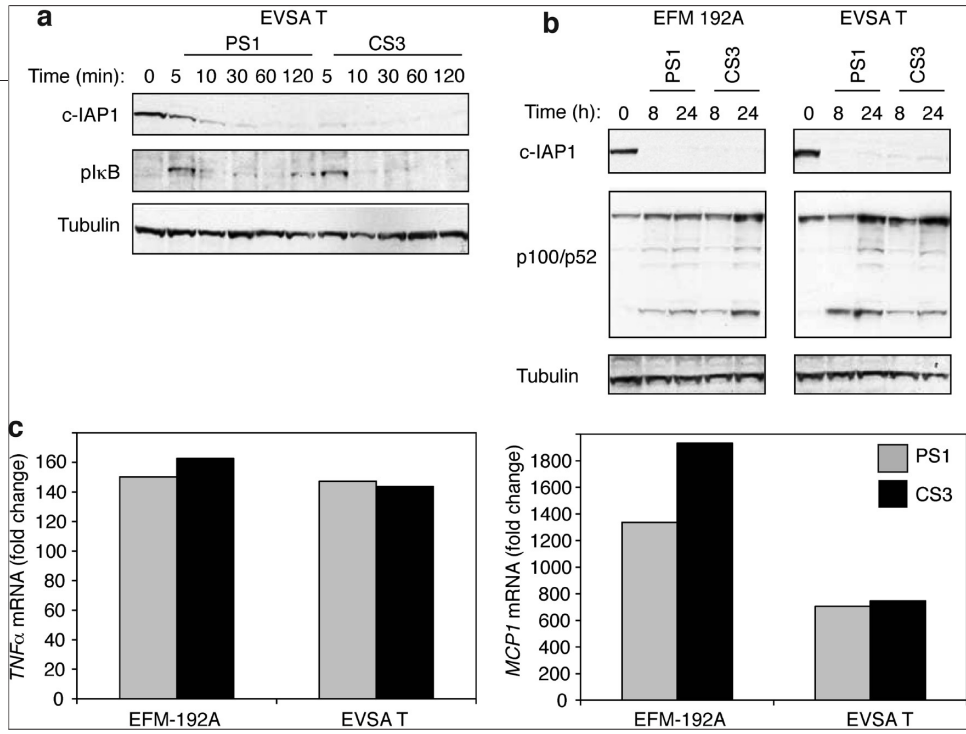

Figure 6. c-IAP-selective and pan-selective IAP antagonists trigger c-IAP1 degradation and NF-κB activation. a) Activation of canonical NF-κB signaling by selective IAP antagonists. EVSA-T cells were treated for the indicated times with PS1 or CS3 (1 μM). The levels of c-IAP1, phosphorylated IκB and Actin were analyzed by Western blotting. b) Selective IAP antagonists induce non-canonical NF-κB signaling. EFM-192A or EVSA-T cells were treated for the indicated periods of time with PS1 or CS3 (1 μM). Protein levels of c-IAP1, p100/p52 and Tubulin were analyzed by Western blotting. c) PS1 and CS3 stimulate *TNFα* and *MCP-1* mRNA expression. Quantitative real-time PCR analysis of *TNFα* and *MCP-1* mRNA expression was done on RNA samples derived from cells treated with PS1 or CS3 (1 μM) for 5 h. All values were normalized to an *RPL19* RNA internal control. These data are representative from three independent experiments.

and 2, and activation of NF-κB pathways leading to production of TNFα play critical roles in initiating the apoptotic process. Our c-IAP-selective antagonists trigger cell death in several tumor cell lines. In addition, these selective reagents also prevent long-term clonogenic survival of tumor cells. However, direct comparison of the c-IAP-selective and the pan-IAP antagonist revealed that the pan-selective antagonist is significantly more effective in stimulating apoptosis and in preventing long-term clonogenic survival of cancer cells. Thus, these results strongly suggest that antagonism of both c-IAP proteins and XIAP is required for efficient induction of apoptosis in cancer cells by IAP antagonists.

Activation of NF-κB signaling pathways is instrumental for IAP antagonist-induced cell death. By comparing the c-IAP-selective and the pan-selective IAP antagonist, we have demonstrated that antagonism of c-IAP proteins is sufficient for the stimulation of proteasomal degradation of c-IAP1 and c-IAP2, and the activation of the canonical and non-canonical NF-κB pathways. Previous studies that used genetic ablation and gene expression down-regulation have shown the role of c-IAP1 and c-IAP2 in these signaling pathways (*30–32, 35, 36*). Findings presented herein demonstrate that pharmacologic targeting of c-IAP proteins leads to NF-κB activation and establish that antagonism of c-IAP proteins, but not XIAP, is essential for this activity of IAP antagonists.

In summary, our study describes c-IAP-selective antagonists as valuable tools in deciphering the mode of action of IAP antagonists in general and supports the development of pan-selective IAP antagonists for efficient induction of cell death and generation of novel therapeutic tools for the treatment of cancer.

METHODS

Cell Lines, Reagents, and Transfections. HEK 293T human embryonic kidney and A2058 melanoma cells were obtained from ATCC. EVSA-T and EFM-192A human breast carcinoma cells were obtained from DSMZ. Transient transfection of HEK 293T cells was done using Geneporter 2 reagent (Genlantis). All cell lines were grown in 50:50 Dulbecco's modified Eagle's and FK12 medium supplemented with 10% FBS, penicillin, and streptomycin. Human recombinant soluble TNFα was from Genentech, Inc. The primary antibodies against c-IAP1 were purchased from R&D (affinity-purified goat antibody); anti-c-IAP2 antibodies were purchased from Abcam; anticaspase-3, -XIAP, and -phospho-specific IκB antibodies were from Cell Signaling Technology, Inc.; anticaspase-9 antibody was from BD Pharmingen; anti-IκB antibodies were from Cell Signaling Technology and Upstate; anti-Flag M2 antibody was from Sigma; anti-Myc antibody was from Roche; anti-p100/p52 antibody was from Upstate Biotechnology; anti-Actin antibody was from ICN Biomedicals; anti-SMAC antibody was from ProSci; MG132 was purchased from Calbiochem; and z-VAD-Fmk was purchased from BioMol.

Molecular Modeling. The models for CS3 and PS1 were generated from an in-house co-crystal structure of c-IAP1 with a compound similar to CS3 (unpublished data). The "Protein Prepara-

tion Wizard" workflow within Maestro 8.0.308 (Schrödinger) was applied to the co-crystal structure. This workflow included the addition of hydrogens and optimization of hydrogen bonds *via* exhaustive sampling of hydrogen positions, as well as minimization of the complex to within 0.30 Å root-mean-square deviation of the starting coordinates. Subsequently, compounds were docked using Glide version 4.5208 (Schrödinger). The grids for docking were generated with default parameters, using the co-crystallized ligand (IAP antagonist) to define the center and size of the binding site. Starting structures for CS3 and PS1 were generated using LigPrep version 2.1207 (Schrödinger), which included ionizing the compounds at physiological pH and generating minimized 3-D conformations. The flexible ligand-docking step was performed using default parameters under Standard Precision mode. The top poses of these compounds made intuitive sense based on crystal structures of other similar compounds. The XIAP coordinates were taken from the published crystal structure of SMAC bound to XIAP BIR3 domain (*21*) (PDB code: 1G73). Superposition of the backbone of XIAP and c-IAP1 was carried out using the "Protein Structure Alignment" tool within Maestro. The aligned protein structures and docked compounds were imported into PyMol version 1.1 (Delano Scientific) to create the figures.

Fluorescence Polarization Binding Assay and Protein Purifications. Fluorescence polarization experiments were performed essentially as described previously (*26, 42*). c-IAP1, c-IAP2, and XIAP BIR3 domain constructs were produced and purified as described previously (*26, 42*).

Viability, Caspase Activity, and Clonogenic Assays. Cells ($1-1.5 \times 10^4$ per well) were seeded into 96-well dishes; 8–12 h later the media were changed, and cells were treated as indicated in the figure legends. Cell viability was measured by neutral red uptake as described (*26, 31*). Caspase-3/7 and Caspase-8 activity assays were performed according to manufacturer's instructions (Promega) as described previously (*26*). Long-term survival (clonogenic) assays were performed as described previously with 200 cells plated on 6-well plates in triplicates after indicated treatments (*31*).

Western Blot Analyses, Immunoprecipitations, and Expression Constructs. Western blot analyses were performed as described previously (*31, 42, 43*) using the following lysis buffer: 1% NP40, 120 mM NaCl, 50 mM Hepes, pH 7.2, 1 mM EDTA, 10% glycerol, protease inhibitory cocktail (Roche). Immunoprecipitations were performed as described previously (*31, 42, 43*). Analyses of canonical and non-canonical NF-κB pathways were performed essentially as described (*31, 36*). Briefly, 12 h before treatment, cells were washed once with PBS, and the growth media were replaced by media containing 2% heat-inactivated FBS. Following treatment cells were lysed in a kinase lysis buffer (20 mM TRIS-HCl, pH 7.5, 150 mM NaCl, 1 mM EDTA, 1% triton, 1× phosphatase inhibitor cocktail II (Sigma)) and analyzed by SDS–PAGE followed by immunoblot analysis, using antiphospho-specific IκB, p100/p52 antibodies and ECL kit (Amersham, NY). Plasmids expressing Flag-XIAP-BIR3, SMAC-Myc and caspase-9 have been described previously (*42*). The region encoding c-IAP BIR1-3 (amino acid residues 1–358) was amplified by PCR and subcloned into p3×Flag-CMV14 vector (Sigma).

Acknowledgment: We thank Alan Olivero, Fred Cohen, Jean-Philippe Stephan, Tatiana Goncharov, members of Protein Engineering and Medicinal Chemistry departments, and the Oligo Synthesis and Sequencing facilities at Genentech that provided help with insightful discussions, suggestions, and reagents. The ALS and the Berkeley Center for Structual Biology are supported by the Department of Energy, National Institutes of Health, and the National Institute of General Medical Sciences. All authors are employees and shareholders of Genentech, Inc.

Supporting Information Available: This material is available free of charge *via* the Internet at http://pubs.acs.org.

REFERENCES

1. Steller, H. (1995) Mechanisms and genes of cellular suicide, *Science 267*, 1445–1449.
2. Thompson, C. B. (1995) Apoptosis in the pathogenesis and treatment of disease, *Science 267*, 1456–1462.
3. Fesik, S. W. (2005) Promoting apoptosis as a strategy for cancer drug discovery, *Nat. Rev. Cancer 5*, 876–885.
4. Ashkenazi, A., and Dixit, V. M. (1998) Death receptors: signaling and modulation, *Science 281*, 1305–1308.
5. Kaufmann, S. H., and Vaux, D. L. (2003) Alterations in the apoptotic machinery and their potential role in anticancer drug resistance, *Oncogene 22*, 7414–7430.
6. Salvesen, G. S., and Abrams, J. M. (2004) Caspase activation—stepping on the gas or releasing the brakes? Lessons from humans and flies, *Oncogene 23*, 2774–2784.
7. Reed, J. C. (2003) Apoptosis-targeted therapies for cancer, *Cancer Cell 3*, 17–22.
8. Hunter, A. M., LaCasse, E. C., and Korneluk, R. G. (2007) The inhibitors of apoptosis (IAPs) as cancer targets, *Apoptosis 12*, 1543–1568.
9. Miller, L. K. (1999) An exegesis of IAPs: salvation and surprises from BIR motifs, *Trends Cell Biol. 9*, 323–832.
10. Salvesen, G. S., and Duckett, C. S. (2002) IAP proteins: blocking the road to death's door, *Nat. Rev. Mol. Cell Biol. 3*, 401–410.
11. Vaux, D. L., and Silke, J. (2005) IAPs, RINGs and ubiquitylation, *Nat. Rev. Mol. Cell Biol. 6*, 287–297.
12. Rothe, M., Pan, M. G., Henzel, W. J., Ayres, T. M., and Goeddel, D. V. (1995) The TNFR2-TRAF signaling complex contains two novel proteins related to baculoviral inhibitor of apoptosis proteins, *Cell 83*, 1243–1252.
13. Wang, C. Y., Mayo, M. W., Korneluk, R. G., Goeddel, D. V., and Baldwin, A. S., Jr. (1998) NF-κB antiapoptosis: induction of TRAF1 and TRAF2 and c-IAP1 and c- IAP2 to suppress caspase-8 activation, *Science 281*, 1680–1683.
14. Eckelman, B. P., Salvesen, G. S., and Scott, F. L. (2006) Human inhibitor of apoptosis proteins: why XIAP is the black sheep of the family, *EMBO Rep 7*, 988–994.
15. Shiozaki, E. N., Chai, J., Rigotti, D. J., Riedl, S. J., Li, P., Srinivasula, S. M., Alnemri, E. S., Fairman, R., and Shi, Y. (2003) Mechanism of XIAP-mediated inhibition of caspase-9, *Mol. Cell 11*, 519–527.
16. Srinivasula, S. M., Hegde, R., Saleh, A., Datta, P., Shiozaki, E., Chai, J., Lee, R. A., Robbins, P. D., Fernandes-Alnemri, T., Shi, Y., and Alnemri, E. S. (2001) A conserved XIAP-interaction motif in caspase-9 and Smac/DIABLO regulates caspase activity and apoptosis, *Nature 410*, 112–116.
17. Du, C., Fang, M., Li, Y., Li, L., and Wang, X. (2000) Smac, a mitochondrial protein that promotes cytochrome c-dependent caspase activation by eliminating IAP inhibition, *Cell 102*, 33–42.
18. Verhagen, A. M., Ekert, P. G., Pakusch, M., Silke, J., Connolly, L. M., Reid, G. E., Moritz, R. L., Simpson, R. J., and Vaux, D. L. (2000) Identification of DIABLO, a mammalian protein that promotes apoptosis by binding to and antagonizing IAP proteins, *Cell 102*, 43–53.
19. Kulathila, R., Vash, B., Sage, D., Cornell-Kennon, S., Wright, K., Koehn, J., Stams, T., Clark, K., and Price, A. (2009) The structure of the BIR3 domain of cIAP1 in complex with the N-terminal peptides of SMAC and caspase-9, *Acta Crystallogr. D, Biol. Crystallogr. 65*, 58–66.
20. Liu, Z., Sun, C., Olejniczak, E. T., Meadows, R. P., Betz, S. F., Oost, T., Herrmann, J., Wu, J. C., and Fesik, S. W. (2000) Structural basis for binding of Smac/DIABLO to the XIAP BIR3 domain, *Nature 408*, 1004–1008.

21. Wu, G., Chai, J., Suber, T. L., Wu, J. W., Du, C., Wang, X., and Shi, Y. (2000) Structural basis of IAP recognition by Smac/DIABLO, *Nature 408*, 1008–1012.
22. Li, L., Thomas, R. M., Suzuki, H., De Brabander, J. K., Wang, X., and Harran, P. G. (2004) A small molecule Smac mimic potentiates TRAIL- and TNFα-mediated cell death, *Science 305*, 1471–1474.
23. Oost, T. K., Sun, C., Armstrong, R. C., Al-Assaad, A. S., Betz, S. F., Deckwerth, T. L., Ding, H., Elmore, S. W., Meadows, R. P., Olejniczak, E. T., Oleksijew, A., Oltersdorf, T., Rosenberg, S. H., Shoemaker, A. R., Tomaselli, K. J., Zou, H., and Fesik, S. W. (2004) Discovery of potent antagonists of the antiapoptotic protein XIAP for the treatment of cancer, *J. Med. Chem. 47*, 4417–4426.
24. Sharma, S. K., Straub, C., and Zawel, L. (2006) Development of peptidomimetics targeting IAPs, *Intl. J. Peptide Res. Ther. 12*, 21–32.
25. Sun, H., Nikolovska-Coleska, Z., Yang, C. Y., Xu, L., Liu, M., Tomita, Y., Pan, H., Yoshioka, Y., Krajewski, K., Roller, P. P., and Wang, S. (2004) Structure-based design of potent, conformationally constrained Smac mimetics, *J. Am. Chem. Soc. 126*, 16686–16687.
26. Zobel, K., Wang, L., Varfolomeev, E., Franklin, M. C., Elliott, L. O., Wallweber, H. J., Okawa, D. C., Flygare, J. A., Vucic, D., Fairbrother, W. J., and Deshayes, K. (2006) Design, synthesis, and biological activity of a potent Smac mimetic that sensitizes cancer cells to apoptosis by antagonizing IAPs, *ACS Chem. Biol. 1*, 525–533.
27. Fulda, S., Wick, W., Weller, M., and Debatin, K. M. (2002) Smac agonists sensitize for Apo2L/TRAIL- or anticancer drug-induced apoptosis and induce regression of malignant glioma *in vivo*, *Nat. Med. 8*, 808–815.
28. Sun, W., Nikolovska-Coleska, Z., Qin, D., Sun, H., Yang, C. Y., Bai, L., Qiu, S., Wang, Y., Ma, D., and Wang, S. (2009) Design, synthesis, and evaluation of potent, nonpeptidic mimetics of second mitochondria-derived activator of caspases, *J. Med. Chem. 52*, 593–596.
29. Vogler, M., Walczak, H., Stadel, D., Haas, T. L., Genze, F., Jovanovic, M., Bhanot, U., Hasel, C., Moller, P., Gschwend, J. E., Simmet, T., Debatin, K. M., and Fulda, S. (2009) Small molecule XIAP inhibitors enhance TRAIL-induced apoptosis and antitumor activity in preclinical models of pancreatic carcinoma, *Cancer Res. 69*, 2425–2434.
30. Bertrand, M. J., Milutinovic, S., Dickson, K. M., Ho, W. C., Boudreault, A., Durkin, J., Gillard, J. W., Jaquith, J. B., Morris, S. J., and Barker, P. A. (2008) cIAP1 and cIAP2 facilitate cancer cell survival by functioning as E3 ligases that promote RIP1 ubiquitination, *Mol. Cell 30*, 689–700.
31. Varfolomeev, E., Blankenship, J. W., Wayson, S. M., Fedorova, A. V., Kayagaki, N., Garg, P., Zobel, K., Dynek, J. N., Elliott, L. O., Wallweber, H. J., Flygare, J. A., Fairbrother, W. J., Deshayes, K., Dixit, V. M., and Vucic, D. (2007) IAP antagonists induce autoubiquitination of c-IAPs, NF-κB activation, and TNFα-dependent apoptosis, *Cell 131*, 669–681.
32. Vince, J. E., Wong, W. W., Khan, N., Feltham, R., Chau, D., Ahmed, A. U., Benetatos, C. A., Chunduru, S. K., Condon, S. M., McKinlay, M., Brink, R., Leverkus, M., Tergaonkar, V., Schneider, P., Callus, B. A., Koentgen, F., Vaux, D. L., and Silke, J. (2007) IAP antagonists target cIAP1 to induce TNFα-dependent apoptosis, *Cell 131*, 682–693.
33. Gaither, A., Porter, D., Yao, Y., Borawski, J., Yang, G., Donovan, J., Sage, D., Slisz, J., Tran, M., Straub, C., Ramsey, T., Iourgenko, V., Huang, A., Chen, Y., Schlegel, R., Labow, M., Fawell, S., Sellers, W. R., and Zawel, L. (2007) A Smac mimetic rescue screen reveals roles for inhibitor of apoptosis proteins in tumor necrosis factor-alpha signaling, *Cancer Res. 67*, 11493–14938.
34. Petersen, S. L., Wang, L., Yalcin-Chin, A., Li, L., Peyton, M., Minna, J., Harran, P., and Wang, X. (2007) Autocrine TNFα signaling renders human cancer cells susceptible to smac-mimetic-induced apoptosis, *Cancer Cell 12*, 445–456.
35. Mahoney, D. J., Cheung, H. H., Mrad, R. L., Plenchette, S., Simard, C., Enwere, E., Arora, V., Mak, T. W., Lacasse, E. C., Waring, J., and Korneluk, R. G. (2008) Both cIAP1 and cIAP2 regulate TNFα-mediated NF-κB activation, *Proc. Natl. Acad. Sci. U.S.A. 105*, 11778–11783.
36. Varfolomeev, E., Goncharov, T., Fedorova, A. V., Dynek, J. N., Zobel, K., Deshayes, K., Fairbrother, W. J., and Vucic, D. (2008) c-IAP1 and c-IAP2 are critical mediators of tumor necrosis factor alpha (TNFα)-induced NF-κB activation, *J. Biol. Chem. 283*, 24295–24299.
37. Franklin, M. C., Kadkhodayan, S., Ackerly, H., Alexandru, D., Distefano, M. D., Elliott, L. O., Flygare, J. A., Mausisa, G., Okawa, D. C., Ong, D., Vucic, D., Deshayes, K., and Fairbrother, W. J. (2003) Structure and function analysis of peptide antagonists of melanoma inhibitor of apoptosis (ML-IAP), *Biochemistry 42*, 8223–8231.
38. Vucic, D. (2008) Targeting IAP (inhibitor of apoptosis) proteins for therapeutic intervention in tumors, *Curr. Cancer Drug Targets 8*, 110–7.
39. Vucic, D., and Fairbrother, W. J. (2007) The inhibitor of apoptosis proteins as therapeutic targets in cancer, *Clin. Cancer Res. 13*, 5995–6000.
40. Varfolomeev, E., and Vucic, D. (2008) (Un)expected roles of c-IAPs in apoptotic and NF-κB signaling pathways, *Cell Cycle 7*, 1511–1521.
41. LaCasse, E. C., Mahoney, D. J., Cheung, H. H., Plenchette, S., Baird, S., and Korneluk, R. G. (2008) IAP-targeted therapies for cancer, *Oncogene 27*, 6252–6275.
42. Vucic, D., Franklin, M. C., Wallweber, H. J., Das, K., Eckelman, B. P., Shin, H., Elliott, L. O., Kadkhodayan, S., Deshayes, K., Salvesen, G. S., and Fairbrother, W. J. (2005) Engineering ML-IAP to produce an extraordinarily potent caspase 9 inhibitor: implications for Smac-dependent anti-apoptotic activity of ML-IAP, *Biochem. J. 385*, 11–20.
43. Varfolomeev, E., Wayson, S. M., Dixit, V. M., Fairbrother, W. J., and Vucic, D. (2006) The inhibitor of apoptosis protein fusion c-IAP2.MALT1 stimulates NF-κB activation independently of TRAF1 AND TRAF2, *J. Biol. Chem. 281*, 29022–29029.